

Hidden entropy production by fast variables

Hyun-Myung Chun¹ and Jae Dong Noh^{1,2}

¹*Department of Physics, University of Seoul, Seoul 130-743, Korea*

²*School of Physics, Korea Institute for Advanced Study, Seoul 130-722, Korea*

(Dated: April 7, 2013)

We investigate nonequilibrium underdamped Langevin dynamics of Brownian particles that interact through a harmonic potential with coupling constant K and are in thermal contact with two heat baths at different temperatures. The system is characterized by a net heat flow and an entropy production in the steady state. We compare the entropy production of the harmonic system with that of Brownian particles linked with a rigid rod. The harmonic system may be expected to reduce to the rigid rod system in the infinite K limit. However, we find that the harmonic system in the $K \rightarrow \infty$ limit produces more entropy than the rigid rod system. The harmonic system has the center of mass coordinate as a slow variable and the relative coordinate as a fast variable. By identifying the contributions of the degrees of freedom to the total entropy production, we show that the hidden entropy production by the fast variable is responsible for the extra entropy production. We discuss the K dependence of each contribution.

PACS numbers: 05.70.Ln, 05.40.-a, 02.50.-r, 05.10.Gg

I. INTRODUCTION

Recent developments in stochastic thermodynamics boost active researches on microscopic systems in thermal environments. Stochastic thermodynamics allows one to define thermodynamic quantities such as heat and work at the microscopic trajectory level, with which thermodynamic properties are readily studied [1, 2].

When one studies a thermodynamic system, a coarse-grained description may be necessary [3–12]. Suppose that some transition rates among microscopic configurations are much faster than the others. Such systems can be coarse-grained in terms of so-called mesostates which refer to a set of microscopic configurations connected via fast processes [4, 8]. The coarse-graining is also necessary if some degrees of freedom are inaccessible due to e.g., a resolution limit of measurement devices [9, 12]. The coarse-graining naturally raises questions on the formulation of effective thermodynamics and on the extent to which the thermodynamic laws are valid.

In this paper, we investigate the entropy production by a harmonic chain of Brownian particles between two heat baths at different temperatures with the focus on the role of fast and slow degrees of freedom. When two heat baths are connected with a medium, heat flows from a higher temperature bath to a lower temperature one and the total entropy increases [13–15]. A toy model for this phenomenon in one dimension was studied thoroughly in Refs. [13, 16] with the equation of motion for the displacement X :

$$M \frac{d^2 X}{dt^2} = -\gamma_1 \frac{dX}{dt} + \xi_1(t) - \gamma_2 \frac{dX}{dt} + \xi_2(t), \quad (1)$$

where γ_i ($i = 1, 2$) is the damping coefficient of a heat bath i at temperature T_i and $\xi_i(t)$ is the thermal Langevin noise satisfying

$$\langle \xi_i(t) \rangle = 0, \quad \langle \xi_i(t) \xi_j(t') \rangle = 2\gamma_i T_i \delta_{ij} \delta(t - t'). \quad (2)$$

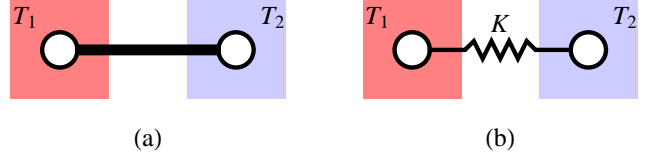


FIG. 1. Comparison of a rigid rod system in (a) and a harmonic system in (b).

The Boltzmann constant k_B is set to unity. The model describes a single Brownian particle of mass M coupled to two heat baths simultaneously. At the same time, as illustrated in Fig. 1(a), it also describes two Brownian particles of total mass M tied with a rigid rod. This rigid rod system was also studied in Refs. [16–18] for the heat conduction in the Feynman ratchet [19].

We notice that the model with a single degree of freedom assumes an ideal medium for heat conduction, which could be realized with a many-body system in the strong coupling limit. A many-body system has multiple degrees of freedom such as the center of mass coordinate and the relative coordinates. In the infinite coupling limit, the relative coordinates relaxing fast can be coarse-grained out to leave the center of mass coordinate as a relevant slow variable. It is interesting to investigate the similarity and the dissimilarity between the system given by (1) and a system with multiple degrees of freedom in the strong coupling limit.

For the purpose, we consider two Brownian particles exchanging a harmonic interaction as shown in Fig. 1(b). Heat conduction and the entropy production in harmonic systems have long been studied [14, 20–25]. In contrast to the previous works, our study focuses on the role of the slow and fast variable. Harmonic systems are analytically tractable [26–31]. We derive the formula for the entropy productions by the slow and fast variables as a function of the coupling constant, which will shed a light on the

effect of the coarse graining.

This paper is organized as follows: The model system consisting of two Brownian particles is introduced in Sec. II. The heat flow and the entropy production in this model are calculated in Sec. III. The slow and fast variable are introduced and their contributions to the total entropy production are investigated in Sec. IV. We compare the harmonic system and the rigid rod system, and draw the conclusion for the hidden entropy production by the fast variable. We conclude the paper with summary and discussions in Sec. V.

II. TWO PARTICLE SYSTEM

Two particles of mass m in one dimension interact through a harmonic potential

$$V(x_1, x_2) = \frac{K}{2}(x_1 - x_2)^2, \quad (3)$$

where x_i ($i = 1, 2$) is the displacement of a particle i and K is the coupling constant. A particle i is in contact with the i th heat bath which is characterized with a temperature T_i and a damping coefficient γ_i (see Fig. 1(b)). The underdamped Langevin equation is given by

$$\begin{aligned} \dot{x}_1 &= v_1, \\ \dot{x}_2 &= v_2, \\ m\dot{v}_1 &= -\gamma_1 v_1 - K(x_1 - x_2) + \xi_1(t), \\ m\dot{v}_2 &= -\gamma_2 v_2 - K(x_2 - x_1) + \xi_2(t), \end{aligned} \quad (4)$$

where $\{\xi_i(t)\}$ represent the thermal noises satisfying (2).

Suppose that the system evolves from a configuration $(x_1, v_1; x_2, v_2)$ at time t to $(x_1 + dx_1, v_1 + dv_1; x_2 + dx_2, v_2 + dv_2)$ in an infinitesimal time step dt . According to stochastic thermodynamics [1], the total entropy production is given by

$$dS_{tot} = dS_s + dS_b, \quad (5)$$

where dS_s denotes the Shannon entropy change of the Brownian particles and dS_b is the entropy change of the thermal heat baths. The latter is given by

$$dS_b = -\frac{dQ_1}{T_1} - \frac{dQ_2}{T_2} \quad (6)$$

where

$$dQ_i = v_i \circ (-\gamma_i v_i dt + dW_i) \quad (7)$$

is the heat absorbed by the Brownian particle from the bath i , and $dW_i \equiv \int_t^{t+dt} dt' \xi_i(t') dt'$ satisfies $\langle dW_i \rangle = 0$ and $\langle (dW_i)^2 \rangle = 2\gamma_i T_i dt$. The notation \circ means that the product is in the Stratonovich sense [32].

The heat can be expressed in different ways. By replacing $(-\gamma_1 v_1 dt + dW_1)$ with $(mdv_1 + K(x_1 - x_2)dt)$, we

obtain

$$\begin{aligned} dQ_1 &= d\left(\frac{1}{2}mv_1^2 + \frac{1}{2}Kx_1^2 - \frac{1}{2}Kx_1x_2\right) \\ &\quad + \frac{K}{2}(x_1v_2 - x_2v_1)dt. \end{aligned} \quad (8)$$

Similarly, we also obtain

$$\begin{aligned} dQ_2 &= d\left(\frac{1}{2}mv_2^2 + \frac{1}{2}Kx_2^2 - \frac{1}{2}Kx_1x_2\right) \\ &\quad - \frac{K}{2}(x_1v_2 - v_1x_2)dt. \end{aligned} \quad (9)$$

They add up to $dE = dQ_1 + dQ_2$, where dE is the change in the total internal energy $E = \frac{1}{2}m(v_1^2 + v_2^2) + V(x_1, x_2)$. The total derivatives in (8) and (9) do not contribute to the steady state average. Hence, the steady-state average of the heat flux, denoted by $q_i \equiv \langle dQ_i/dt \rangle_s$ is given by

$$q = q_1 = -q_2 = \frac{K}{2} \langle x_1v_2 - x_2v_1 \rangle_s, \quad (10)$$

where $\langle \cdot \rangle_s$ means the steady state ensemble average.

The heat flux acquires an interesting interpretation by regarding x_i and v_i as the coordinates of the position vector $\mathbf{x} = (x_1, x_2, 0)$ and the velocity vector $\mathbf{v} = (v_1, v_2, 0)$ of an imaginary particle moving on a xy plane in a three dimensional space. Then the heat flux in (10) becomes proportional to the z component of the angular momentum $\mathbf{L} = m\mathbf{x} \times \mathbf{v}$ of the imaginary particle:

$$q = \frac{K}{2m} \langle L_3 \rangle_s. \quad (11)$$

A nonzero heat flow implies a rotational motion. Such a rotational motion induced by a nonequilibrium driving was investigated in the context of a Brownian gyration [33].

We find another useful expression for the heat flow. The Stratonovich product $v_1 \circ dW_1$ in (7) is defined as $\frac{1}{2}[v_1 + (v_1 + dv_1)]dW_1$ [32], where $dv_1 = [-\gamma_1 v_1 dt - K(x_1 - x_2)dt + dW_1]/m$ from the Langevin equation. The ensemble average yields $\langle v_1 \circ dW_1 \rangle = \frac{\gamma_1 T_1}{m} dt$. Thus, the average heat flux in the steady state can be written as

$$q = \frac{2\gamma_1}{m} \left(\frac{T_1}{2} - \frac{1}{2}m \langle v_1^2 \rangle_s \right). \quad (12)$$

The heat flow is driven by the imbalance between the temperature of the heat bath and the effective temperature of the particle measured by the kinetic energy. Note that the expression (12) is valid not only in the steady state but also in a transient state.

In the steady state, the Shannon entropy of the particles does not change ($\langle dS_s \rangle_s = 0$). Consequently, the total entropy production rate in the steady state is given by

$$s \equiv \left\langle \frac{dS_{tot}}{dt} \right\rangle_s = \frac{-q}{T_1} + \frac{q}{T_2} = \left(\frac{1}{T_2} - \frac{1}{T_1} \right) q. \quad (13)$$

The heat flux and the entropy production rate is proportional to each other.

III. HEAT FLOW AND ENTROPY PRODUCTION

For the heat flux, we need to evaluate the second moments of the velocities, $M_{ij} \equiv \langle v_i(t)v_j(t) \rangle_s$. The model with the linear Langevin equation in (4) belongs to the class of the multivariate Ornstein-Uhlenbeck process [32]. The second moments of such a system satisfy a set of linear equations [32], from which M_{ij} can be easily evaluated. Instead of using the method, we evaluate the moments explicitly for self-containedness.

The Langevin equation (4) is solved in the Fourier space. We introduce column vectors $\tilde{\mathbf{x}}(\omega) = (\tilde{x}_1(\omega), \tilde{x}_2(\omega))^T$ and $\tilde{\boldsymbol{\xi}}(\omega) = (\tilde{\xi}_1(\omega), \tilde{\xi}_2(\omega))^T$ with $\tilde{x}_i(\omega) = \int_{-\infty}^{\infty} dt e^{i\omega t} x_i(t)$ and $\tilde{\xi}_i(\omega) = \int_{-\infty}^{\infty} dt e^{i\omega t} \xi_i(t)$. The superscript T denotes the transpose. The Fourier components of the thermal noise obey

$$\langle \tilde{\xi}_i(\omega) \rangle = 0, \quad \langle \tilde{\xi}_i(\omega) \tilde{\xi}_j(\omega') \rangle = 4\pi\gamma_i T_i \delta_{ij} \delta(\omega + \omega'). \quad (14)$$

The Langevin equation becomes $\mathbf{F}(\omega)\tilde{\mathbf{x}}(\omega) = \tilde{\boldsymbol{\xi}}(\omega)$, where $\mathbf{F}(\omega)$ is a 2×2 matrix given by

$$\mathbf{F}(\omega) = \begin{pmatrix} -m\omega^2 - i\gamma_1\omega + K & -K \\ -K & -m\omega^2 - i\gamma_2\omega + K \end{pmatrix}.$$

The steady state solution is given by $\tilde{\mathbf{x}}(\omega) = \mathbf{F}(\omega)^{-1}\tilde{\boldsymbol{\xi}}(\omega)$. The homogeneous solution is ignored because it vanishes in the steady state. For convenience, we write the solution as $\tilde{\mathbf{x}}(\omega) = \frac{1}{D(\omega)}\mathbf{C}(\omega)\tilde{\boldsymbol{\xi}}(\omega)$ where

$$D(\omega) = (-m\omega^2 - i\gamma_1\omega + K)(-m\omega^2 - i\gamma_2\omega + K) - K^2 \quad (15)$$

is the determinant of $\mathbf{F}(\omega)$ and $\mathbf{C}(\omega) = \mathbf{C}(\omega)^T$ is the co-factor matrix given by

$$\mathbf{C}(\omega) = \begin{pmatrix} -m\omega^2 - i\gamma_2\omega + K & K \\ K & -m\omega^2 - i\gamma_1\omega + K \end{pmatrix}. \quad (16)$$

By using $\tilde{v}_i(\omega) = -i\omega\tilde{x}_i(\omega)$ and the noise correlations in (14), we can write

$$M_{ij} = \int_{-\infty}^{\infty} \frac{d\omega}{\pi} \frac{\omega^2 [\sum_l \gamma_l T_l C_{il}(\omega) C_{jl}(-\omega)]}{D(\omega)D(-\omega)}. \quad (17)$$

This integral is evaluated using the contour integral method, as detailed in Appendix A. The results are

$$\begin{aligned} M_{11} &= \frac{T_1}{m} - \frac{\gamma_2 K (T_1 - T_2)}{(\gamma_1 + \gamma_2)(Km + \gamma_1\gamma_2)}, \\ M_{22} &= \frac{T_2}{m} + \frac{\gamma_1 K (T_1 - T_2)}{(\gamma_1 + \gamma_2)(Km + \gamma_1\gamma_2)}, \\ M_{12} &= M_{21} = 0. \end{aligned} \quad (18)$$

Inserting these into (12), we finally obtain

$$q = \frac{\gamma_1\gamma_2 K (T_1 - T_2)}{(\gamma_1 + \gamma_2)(Km + \gamma_1\gamma_2)} \quad (19)$$

for the heat flux and

$$s = \frac{\gamma_1\gamma_2 K}{(\gamma_1 + \gamma_2)(Km + \gamma_1\gamma_2)} \frac{(T_1 - T_2)^2}{T_1 T_2} \quad (20)$$

for the entropy production rate.

The heat flow is nonzero when $T_1 \neq T_2$ and K is nonzero. The system absorbs a heat from a higher temperature heat bath and dissipates to a lower temperature one, which increases the entropy of the whole system.

IV. HIDDEN ENTROPY PRODUCTION

The heat flux and the entropy production rate increase monotonically with the coupling constant K . In the $K \rightarrow \infty$ limit, the heat flow rate converges to

$$q_\infty \equiv \lim_{K \rightarrow \infty} q = \frac{\gamma_1\gamma_2}{m(\gamma_1 + \gamma_2)} (T_1 - T_2), \quad (21)$$

and the entropy production rate converges to

$$s_\infty = \frac{\gamma_1\gamma_2}{m(\gamma_1 + \gamma_2)} \frac{(T_1 - T_2)^2}{T_1 T_2}. \quad (22)$$

In this limit, the relative displacement of the two particles ($|x_2 - x_1| \sim K^{-1/2}$) vanishes. Hence, one may regard the limiting case as the rigid rod system, that is, a single Brownian particle of mass $M = 2m$ (see Fig. 1). It is worthy to compare the heat flux in both cases. The heat flux q_{rigid} of the rigid rod system is given by Ref. [13, 16]

$$q_{\text{rigid}} = \frac{\gamma_1\gamma_2}{M(\gamma_1 + \gamma_2)} (T_1 - T_2) = \frac{\gamma_1\gamma_2}{2m(\gamma_1 + \gamma_2)} (T_1 - T_2). \quad (23)$$

Surprisingly, the heat flux q_{rigid} is the half of the limiting values q_∞ because of the factor 2 in the denominator.

In order to understand the origin of the discrepancy, we rewrite the Langevin equation (4) in terms of the center of mass coordinate $X = (x_1 + x_2)/2$ and the relative coordinate $x = x_1 - x_2$. The equations of motion for X and x are given by

$$\begin{aligned} \dot{X} &= V, \\ \dot{x} &= v, \\ M\dot{V} &= -(\gamma_1 + \gamma_2)V - \frac{(\gamma_1 - \gamma_2)}{2}v + \zeta_1(t), \\ \mu\dot{v} &= -\frac{(\gamma_1 + \gamma_2)}{4}v - \frac{(\gamma_1 - \gamma_2)}{2}V - Kx + \zeta_2(t), \end{aligned} \quad (24)$$

where $M = 2m$ is the total mass, $\mu = m/2$ is the reduced mass, $\zeta_1 \equiv \xi_1 + \xi_2$ obeying $\langle \zeta_1(t) \rangle = 0$ and $\langle \zeta_1(t)\zeta_1(t') \rangle = 2(\gamma_1 T_1 + \gamma_2 T_2)\delta(t - t')$, and $\zeta_2 \equiv (\xi_1 - \xi_2)/2$ obeying $\langle \zeta_2(t) \rangle = 0$ and $\langle \zeta_2(t)\zeta_2(t') \rangle = \frac{1}{2}(\gamma_1 T_1 + \gamma_2 T_2)\delta(t - t')$. The center of mass and the relative coordinates are coupled through the noise correlation $\langle \zeta_1(t)\zeta_2(t') \rangle = (\gamma_1 T_1 - \gamma_2 T_2)\delta(t - t')$ and the friction forces.

We can grasp an important feature of the system by considering the case with $\gamma_1 = \gamma_2 = \gamma$. The center of

mass performs a Brownian motion with the effective temperature $T_{\text{eff}} = (T_1 + T_2)/2$, and the relative coordinate performs the Ornstein-Uhlenbeck process [32] under the harmonic potential $\frac{1}{2}Kx^2$ with the same effective temperature T_{eff} . The center of mass coordinate diffuses with the time scale $\tau_X \sim m/\gamma$. The relative coordinate oscillates with the time scale $\tau_x \sim \sqrt{m/K}$ with the amplitude $|x| \sim \sqrt{T_{\text{eff}}/K}$. Therefore, in the $K \rightarrow \infty$ limit, x becomes a *fast* variable ($\tau_x \ll \tau_X$) and becomes frozen ($|x| \rightarrow 0$) in amplitude, while X becomes a *slow* variable being governed by the same equation of motion in (1) as the rigid rod system.

Although the fast variable x becomes frozen in the $K \rightarrow \infty$ limit, it may leave a signature in thermodynamic quantities. We scrutinize this possibility by decomposing the heat flux, or equivalently the entropy production rate, into the sum of contributions of the fast and the slow variables. We start with the expression (8) for general γ_1 and γ_2 . After inserting $v_1 = V + v/2$ into (8), we obtain

$$dQ_1 = (-\gamma_1 V^2 dt + V \circ dW_1) + (-\gamma_1 v V dt + \left(-\frac{\gamma_1}{4} v^2 dt + \frac{v}{2} \circ dW_1\right)) . \quad (25)$$

Each term corresponds to the heat flow via the slow variable, the interplay between the slow and fast variables, and the fast variable, respectively. Thus, the average heat flow rate in the steady state is decomposed as

$$q = q_S + q_F + q_m , \quad (26)$$

where

$$q_S = \frac{2\gamma_1}{M} \left(\frac{T_1}{2} - \frac{1}{2} M \langle V^2 \rangle_s \right) \quad (27)$$

is the contribution from the slow variable,

$$q_F = \frac{\gamma_1}{2\mu} \left(\frac{T_1}{2} - \frac{1}{2} \mu \langle v^2 \rangle_s \right) \quad (28)$$

is from the fast variable, and

$$q_m = -\gamma_1 \langle vV \rangle_s \quad (29)$$

is the mixed contribution.

Each contribution is easily evaluated using the second moments M_{ij} obtained in (18). For example, $\langle V^2 \rangle_s = (M_{11} + 2M_{12} + M_{22})/4$. The results are

$$q_S = \frac{\gamma_1 \gamma_2}{4m} \frac{2Km + \gamma_1^2 + \gamma_1 \gamma_2}{(\gamma_1 + \gamma_2)(Km + \gamma_1 \gamma_2)} (T_1 - T_2) \quad (30)$$

$$q_m = -\frac{\gamma_1}{2m} \frac{\gamma_1 \gamma_2}{(Km + \gamma_1 \gamma_2)} (T_1 - T_2) \quad (31)$$

$$q_F = q_S . \quad (32)$$

Surprisingly, the fast variable contributes to the heat flow by the same amount as the slow variable at all values of K . This hidden entropy production by the fast variable explains the discrepancy between q_∞ and q_{rigid} . The

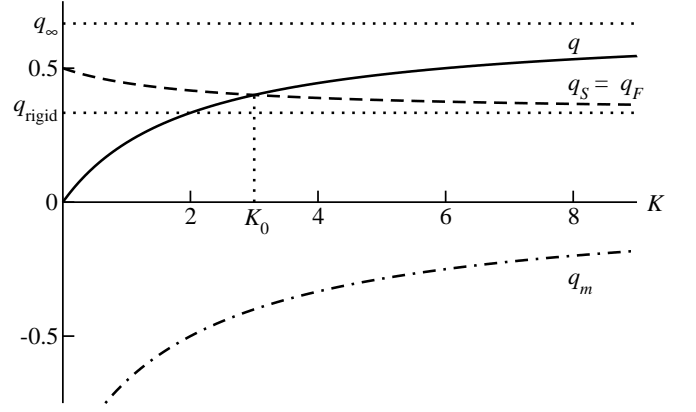


FIG. 2. Heat flow rates as a function of K . Parameter values are $\gamma_1 = 2$, $\gamma_2 = 1$, $m = 1$, and $(T_1 - T_2) = 1$.

mixed contribution q_m has the opposite sign to q_S and q_F , and vanishes in the infinite coupling limit. They are plotted as a function of K in Fig. 2.

Measurements are done within the resolution limit of probing devices. Suppose that one experiments on the harmonic system with large K with a device whose time resolution $\tau_{\text{res}} \gg \tau_x$. Then, the harmonic system would be observed as the rigid rod system. Measurements would yield the apparent entropy production from the slow variable only, which is a part of the total entropy production.

The opposite case is also interesting. When the coupling constant vanishes ($K \rightarrow 0$), the two particles are in their own thermal equilibrium and the heat flux and the entropy production vanish. However, the apparent heat flux q_S associated with the center of mass coordinate still remains finite even at $K = 0$. Suppose that the two noninteracting particles are confined by an external potential within a region whose size is much smaller than the spatial resolution of an experimental device. Then, the two particles would be considered as a single particle, which results in the overestimation of the total entropy production.

The results are summarized in Fig. 2. The heat flux q increases from 0 to q_∞ as K increases from zero to infinity. The apparent heat flux q_S is different from q . When K is small, the hidden heat flux ($q_F + q_m$) is negative so that the resolution limited measurement would overestimate the entropy production. When K is large, the hidden heat flux is positive so that the resolution limited measurement would underestimate the entropy production. The threshold K_0 is determined from the condition $q = q_S$, which yields that

$$K_0 = \frac{\gamma_1(\gamma_1 + \gamma_2)}{2m} . \quad (33)$$

The conclusion on the hidden entropy production does not depend on the specific form of the interaction potential $V(x_1, x_2)$. We also considered the system with $V(x_1, x_2) = \frac{K}{2}(x_1 - x_2)^2 + \frac{1}{2}kx_1^2 + \frac{1}{2}kx_2^2$. That is, each

particle is trapped with the additional harmonic potential with the coupling constant k . This case is also analyzed in Appendix A. The total heat flux and the components are given in (A5). With this setting, we also obtain the same result that $q = 2q_{\text{rigid}}$ and that $q_S = q_F = q_{\text{rigid}}$ with $q_m = 0$ in the $K \rightarrow \infty$ limit.

V. SUMMARY AND DISCUSSIONS

We have investigated the role of a fast variable in the entropy production. For the harmonic system, the total entropy production is separated into the contributions from the slow variable (center of mass coordinate) and the fast variable (relative coordinate), and the mixed contribution. We found that the hidden entropy production due to the fast variable remains finite even in the infinite coupling limit.

Our study reveals the difference between the rigid rod system and the harmonic system in the infinite coupling limit. In the former system, the relative coordinate $x = x_1 - x_2$ is constrained to be zero without any dynamic fluctuations. In the latter system, the amplitude of the relative motion is also negligible ($x \sim \mathcal{O}(K^{-1/2})$). However, the velocity fluctuations are non-negligible, which results in a finite additional hidden entropy production.

The hidden entropy production could be relevant for heat engines. When one models a heat engine, some degrees of freedom may be ignored for the sake of simplicity. For example, in the Feynman ratchet, vanes and a ratchet are assumed to be linked with a rigid axle [17–19], which ignore relative motions of the two parts. Our results suggest that the entropy production in such a model should be less than the actual one because of the hidden entropy. The entropy production is the origin for the loss in the efficiency of a heat engine. Our result warns that all the fast variables should be taken into account in analyzing the efficiency of a heat engine.

Appendix A: Evaluation of the integral in (17)

The denominator (numerator) of the integrand in (17) is the 8th (6th) degree polynomial in ω . Thus, one can add a half-circular contour of the infinite radius in the complex ω plane to make a closed contour as shown in Fig. 3. The contour integral is determined by the residues of the poles that are located at the roots of $D(\omega)$ and $D(-\omega)$ inside the contour.

We first consider the roots of the quartic polynomial $D(\omega)$. A trivial root is located at $\omega = 0$. The others are the solutions of $g(\omega) \equiv m^2\omega^3 + im(\gamma_1 + \gamma_2)\omega^2 - (\gamma_1\gamma_2 + 2mK)\omega - i(\gamma_1 + \gamma_2)K = 0$. It is more convenient to work with $\tilde{g}(\Omega) \equiv ig(\omega = i\Omega) = m^2\Omega^3 + m(\gamma_1 + \gamma_2)\Omega^2 + (\gamma_1\gamma_2 + 2mK)\Omega + (\gamma_1 + \gamma_2)K$ whose coefficients are real and positive. Positivity of coefficients guarantees that real positive roots do not exist and that one of the roots, denoted by Ω_1 , must be real and negative. The

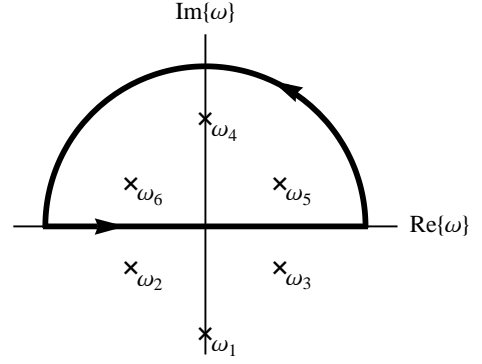


FIG. 3. Integration contour for the evaluation of (17) in complex ω plane. Simple poles are marked with \times symbols. The non-zero roots $\omega_{4,5,6}$ of $D(-\omega)$ are in the upper half-plane, while the non-zero roots $\omega_{1,2,3}$ of $D(\omega)$ are in the lower half-plane.

remaining two roots, denoted by Ω_2 and Ω_3 , may be real and negative, or a pair of complex conjugates. In order to determine whether they are inside the contour in Fig. 3, we need to know the sign of the real parts of Ω_2 and Ω_3 . The three roots of $\tilde{g}(\Omega)$ satisfy $\Omega_1 + \Omega_2 + \Omega_3 = -(\gamma_1 + \gamma_2)/m$. Note that $\tilde{g}(-(\gamma_1 + \gamma_2)/m) = -(\gamma_1\gamma_2 + mK)(\gamma_1 + \gamma_2)/m < 0$ and that $\tilde{g}(x) > 0$ for any real $x > 0$. This implies that $\Omega_1 > -(\gamma_1 + \gamma_2)/m$ and $\text{Re}\{\Omega_{2,3}\} < 0$. Consequently, the nonzero roots $\omega_k = i\Omega_k$ ($k = 1, 2, 3$) of $D(\omega)$ are located in the lower half-plane. The nonzero roots $\omega_{3+k} = -\omega_k$ ($k = 1, 2, 3$) of $D(-\omega)$ are located in the upper half-plane (see Fig. 3).

We identified all the roots of $D(\omega)D(-\omega)$. Among them the degenerate root $\omega = 0$ do not contribute to the integral in (17) because it is canceled with ω^2 in the numerator of the integrand. The contour in Fig. 3 includes only ω_4 , ω_5 , and ω_6 . Therefore, the integral in (17) is equal to

$$M_{ij} = 2\pi i [\text{Res}(\omega_4) + \text{Res}(\omega_5) + \text{Res}(\omega_6)], \quad (\text{A1})$$

where $\text{Res}(\omega_k)$ denotes the residue of the integrand function in (17) at the simple pole ω_k . The roots and the residues are easily evaluated by using a software capable of symbolic algebra, which yields the results in (18).

We can generalize the analysis to the system with the potential energy

$$V(x_1, x_2) = \frac{k}{2}(x_1^2 + x_2^2) + \frac{K}{2}(x_1 - x_2)^2 \quad (\text{A2})$$

instead of the potential energy in (3). For simplicity, we set $\gamma_1 = \gamma_2 = \gamma$. This system has the modified matrix $F(\omega)$ whose elements are $F_{11}(\omega) = F_{22}(\omega) = -m\omega^2 - i\gamma\omega + k + K$ and $F_{12}(\omega) = F_{21}(\omega) = -K$. Then, $D(\omega) = \det F(\omega)$ has four roots at

$$\begin{aligned} \omega_{1,2} &= [-i\gamma \pm \sqrt{4mk - \gamma^2}]/(2m), \\ \omega_{3,4} &= [-i\gamma \pm \sqrt{4m(k + 2K) - \gamma^2}]/(2m) \end{aligned} \quad (\text{A3})$$

in the lower half-plane, and $D(-\omega)$ has four roots at $\omega_{4+j} = -\omega_j$ ($j = 1, \dots, 4$) in the upper half-plane. Therefore, the integral corresponding to (17) is determined by the residues at $\omega_{5,6,7,8}$. The results are

$$\begin{aligned} M_{11} &= \frac{T_1}{m} - \frac{K^2(T_1 - T_2)}{2\{mK^2 + \gamma^2(k + K)\}}, \\ M_{22} &= \frac{T_2}{m} + \frac{K^2(T_1 - T_2)}{2\{mK^2 + \gamma^2(k + K)\}}, \\ M_{12} &= M_{21} = 0. \end{aligned} \quad (\text{A4})$$

Inserting these into Eqs. (12), (27), (28), and (29), we obtain that

$$\begin{aligned} q &= \frac{\gamma K^2}{2\{mK^2 + \gamma^2(k + K)\}}(T_1 - T_2), \\ q_S &= q_F = \frac{\gamma}{4m}(T_1 - T_2), \\ q_m &= -\frac{\gamma}{2m} \frac{\gamma^2(k + K)}{\{mK^2 + \gamma^2(k + K)\}}(T_1 - T_2). \end{aligned} \quad (\text{A5})$$

In the $K \rightarrow \infty$ limit, we obtain that $q_m \rightarrow 0$ and $q_S = q_F \rightarrow q_\infty/2 = q_{\text{rigid}}$.

ACKNOWLEDGMENTS

This work was supported by the Basic Science Research Program through the NRF Grant No. 2013R1A2A2A05006776.

-
- [1] U. Seifert, Phys. Rev. Lett. **95**, 040602 (2005).
 - [2] K. Sekimoto, Prog Theor Phys Suppl **130**, 17 (1998).
 - [3] F. Zamponi, F. Bonetto, L. F. Cugliandolo, and J. Kurchan, J. Stat. Mech.: Theor. Exp. **2005**, P09013 (2005).
 - [4] S. Rahav and C. Jarzynski, J. Stat. Mech.: Theor. Exp. **2007**, P09012 (2007).
 - [5] S. Pigolotti and A. Vulpiani, J. Chem. Phys. **128**, 154114 (2008).
 - [6] A. Puglisi, S. Pigolotti, L. Rondoni, and A. Vulpiani, J. Stat. Mech.: Theor. Exp. **2010**, P05015 (2010).
 - [7] M. Santillan and H. Qian, Phys. Rev. E **83**, 041130 (2011).
 - [8] M. Esposito, Phys. Rev. E **85**, 041125 (2012).
 - [9] J. Mehl, B. Lander, C. Bechinger, V. Blickle, and U. Seifert, Phys. Rev. Lett. **108**, 220601 (2012).
 - [10] K. Kawaguchi and Y. Nakayama, Phys. Rev. E **88**, 022147 (2013).
 - [11] Y. Baek, M. Ha, H. Jeong, and H. Park, arXiv (2014), 1402.1235v3.
 - [12] N. Shiraishi and T. Sagawa, Phys. Rev. E **91**, 012130 (2015).
 - [13] P. Visco, J. Stat. Mech.: Theor. Exp. **2006**, P06006 (2006).
 - [14] A. Kundu, S. Sabhapandit, and A. Dhar, J. Stat. Mech.: Theor. Exp. **2011**, P03007 (2011).
 - [15] H. C. Fogedby and A. Imparato, J. Stat. Mech.: Theor. Exp. **2011**, P05015 (2011).
 - [16] C. Van den Broeck, E. Kestemont, and M. M. Mansour, Europhysics Letters **56**, 771 (2001).
 - [17] J. Parrondo and P. Español, Am. J. Phys. **64**, 1125 (1996).
 - [18] A. Gomez-Marin and J. Sancho, Phys. Rev. E **73**, 045101(R) (2006).
 - [19] R. P. Feynman, R. B. Leighton, and M. Sands, *The Feynman Lectures on Physics*, vol. 1 (Addison Wesley, Reading, MA, 1963).
 - [20] Z. Rieder, J. Math. Phys. **8**, 1073 (1967).
 - [21] C. Bernardin, V. Kannan, J. L. Lebowitz, and J. Lukkarinen, J Stat Phys **146**, 800 (2012).
 - [22] A. Dhar, K. Venkateshan, and J. Lebowitz, Phys. Rev. E **83**, 021108 (2011).
 - [23] S. Sabhapandit, Phys. Rev. E **85**, 021108 (2012).
 - [24] K. Saito and A. Dhar, Phys. Rev. E **83**, 041121 (2011).
 - [25] H. C. Fogedby and A. Imparato, J. Stat. Mech.: Theor. Exp. **2012**, P04005 (2012).
 - [26] C. Kwon, J. D. Noh, and H. Park, Phys. Rev. E **83**, 061145 (2011).
 - [27] C. Kwon, J. D. Noh, and H. Park, Phys. Rev. E **88**, 062102 (2013).
 - [28] J. D. Noh, J. Stat. Mech.: Theor. Exp. **2014**, P01013 (2014).
 - [29] J. D. Noh and J.-M. Park, Phys. Rev. Lett. **108**, 240603 (2012).
 - [30] J. D. Noh, C. Kwon, and H. Park, Phys. Rev. Lett. **111**, 130601 (2013).
 - [31] S. Ciliberto, N. Garnier, S. Hernandez, C. Lacpatia, J. F. Pinton, and G. Ruiz Chavarria, Physica A: Statistical Mechanics and its Applications **340**, 240 (2004).
 - [32] C. Gardiner, *Stochastic Methods*, A Handbook for the Natural and Social Sciences (Springer, 2010).
 - [33] R. Filliger and P. Reimann, Phys. Rev. Lett. **99**, 230602 (2007).